RF Transceivers Enable Forced Spurious Decorrelation in Digital Beamforming Phased Arrays

Peter Delos, Michael Jones, and Mark Robertson
Analog Devices, Inc.

Introduction

In large digital beamforming antennas, dynamic range improvements through the beamforming process of combining signals from distributed waveform generators and receivers is highly desirable. A 10logN dynamic range improvement can be obtained in both noise and spurious performance if the associated error terms are uncorrelated. N in this case is the number of waveform generator or receiver channels. Noise by nature is a very random process and therefore lends itself well to tracking correlated and uncorrelated noise sources. However, spurious signals make it less obvious how to force spurs to be uncorrelated. Therefore, any design method that can force spurious signals to be uncorrelated is valuable to phased array system architecture.

In this article we review a previously published technique to force spurious signals to be uncorrelated by offsetting the LO frequencies and digitally compensating for this offset. We then show how the most recent Analog Devices transceiver product, the ADRV9009, has built-in features enabling this capability. We then conclude with measured data demonstrating the results of the technique.

Known Spurious Decorrelation Methods

Various methods to force spurious decorrelation in phased arrays have been known for some time. Our first known publication dates back to 2002,[1] where a general method to ensure receiver spurious are uncorrelated is described. In the approach, signals are first modified in a known way from receiver to receiver. Then the signals become distorted by the receiver's nonlinear components. At the receiver output, the modifications introduced earlier in the receiver are inverted. The intended signals become coherent or correlated, but the distorted terms are not restored. The modification method implemented in their testing was to set each local oscillator (LO) synthesizer to a different frequency, then correct for the modification by digitally tuning numerically controlled oscillators (NCOs) in the digital processing. Several other methods have also been published.[2,3]

Years later, with the advanced integration of full transceiver subsystems in single monolithic silicon, embedded programmable features in the transceiver products enable the spurious decorrelation method described in the article "Correlation of Nonlinear Distortion in Digital Phased Arrays: Measurement and Mitigation."[1]

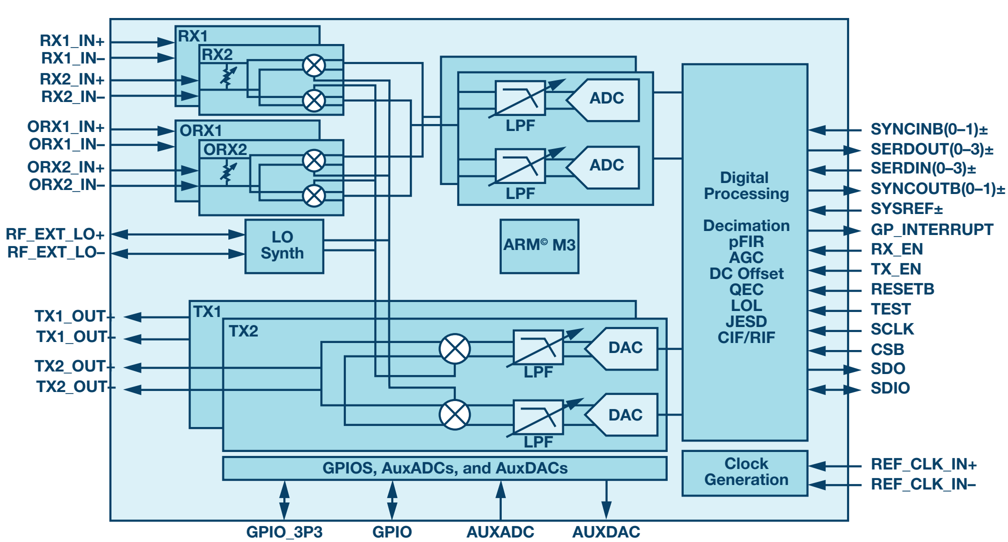

Figure 1. ADRV9009 functional block diagram.

Transceiver Features Enabling Spurious Decorrelation

A functional block diagram of the Analog Devices transceiver ADRV9009 is shown in Figure 1.

Each waveform generator or receiver is implemented with a direct conversion architecture. Daniel Rabinkin's article, "Front-End Nonlinear Distortion and Array Beamforming," discusses direct conversion architectures at greater length.[4] The LO frequencies can be programmed independently on each IC. The digital processing section includes digital up/down conversion with NCOs that can also be programmed independently across ICs. Peter Delos' article, "A Review of Wideband RF Receiver Architecture Options," provides further description of digital downconversion.[5]

Next, we will demonstrate a method to force spurious decorrelation across multiple transceivers. First, the LOs are offset in frequency by programming the on-board phase-locked loops (PLLs). Then the NCO frequencies are set to digitally compensate for the applied LO frequency offset. By adjusting both features inside the transceiver IC, the digital data to and from the transceivers does not have to be offset in frequency and the entire frequency translation and spurious decorrelation is built into the transceiver IC.

A representative block diagram for an array of waveform generators is shown in Figure 2. In our description we will describe the method and show data for waveform generators, but the method is equally applicable to an array of receivers.

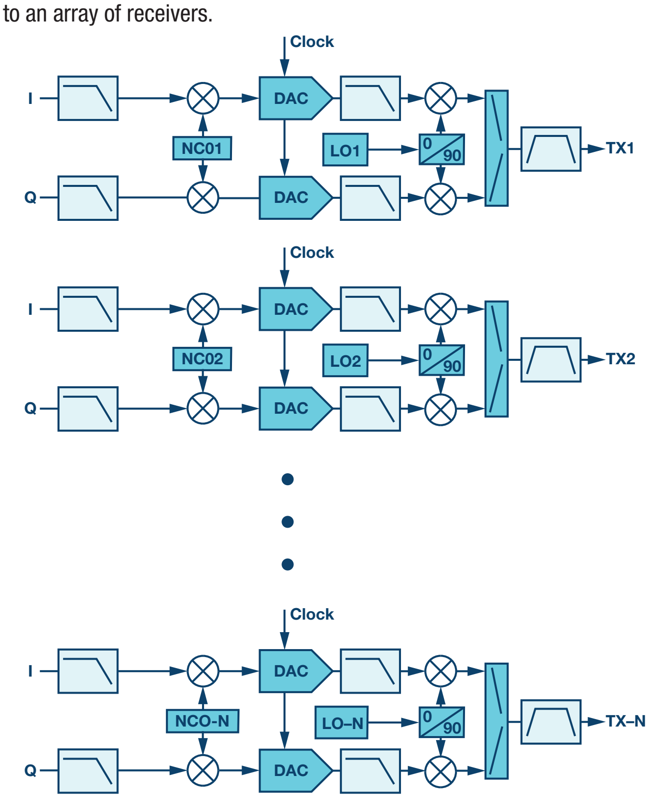

Figure 2. Forcing spurious to be uncorrelated by programming LO and NCO frequencies across an array of waveform generators.

To illustrate the concept in frequency, an example with two transmit signals from a direct conversion architecture is shown in Figure 3. These cases are shown where the RF is on the high side of the LO. In a direct conversion architecture, the image frequency and third harmonic appear on the opposite side of the LO and are shown below the LO frequency. When the LO frequencies are set to the same frequency across channels, the spurious frequencies are also at the same frequencies, as shown in Figure 3a. Figure 3b illustrates a case where LO2 is set at a higher frequency than LO1. The digital NCOs are equally offset such that the RF signal achieves coherent gain. The images and third-harmonic distortion products are at different frequencies and thus uncorrelated. Figure 3c illustrates the same configuration as Figure 3b but adds modulation to the RF carrier.

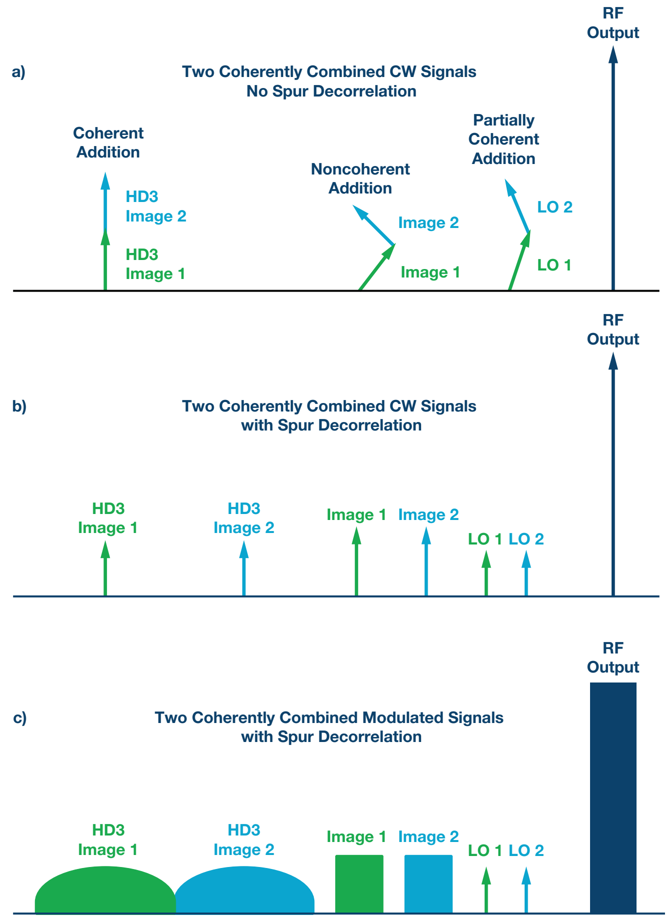

Figure 3. Spectral illustration showing the spurious signals in frequency. Three cases are shown: (a) Two combined CW signals with no spur decorrelation, (b) two combined CW signals with forced spur decorrelation, and (c) two combined modulated signals with forced spur decorrelation.

Measured Results

An 8-channel, transceiver-based RF testbed was assembled to evaluate the transceiver product line for phased array applications. The test setup for evaluating the waveform generators is shown in Figure 4. For this test, the same digital data is applied to all waveform generators. A calibration is performed across the channels by adjusting the NCO phase to ensure the RF signals are in phase at the 8-way combiner and coherently combine.

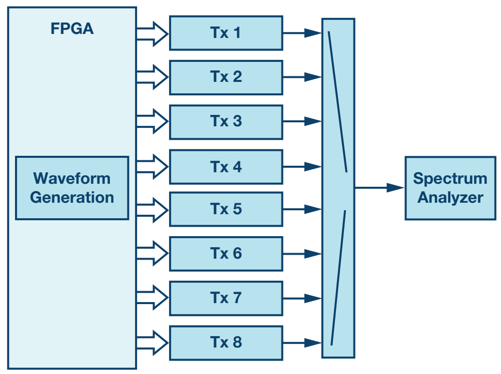

Figure 4. Waveform generator spurious test setup.

Next we will show test data comparing spurious with the LOs and NCOs all set to the same frequency vs. spurious when the LOs and NCOs are offset in frequency. The transceivers used share an LO within a 2-channel device (see Figure 1), so for the eight RF channels there are four different LO frequencies.

In Figure 5 and Figure 6, the transceiver NCOs and LOs are all set to the same frequency. In this case, the spurious signals produced from the image, the LO leakage, and the third harmonic are all at the same frequency. Figure 5 shows the individual transmit outputs measured on a spectrum analyzer. Figure 6 shows the combined output. In this particular test the spurs of the image and the LO leakage measured in dBc relative to the carrier showed improvement, but the third harmonic did not improve. In our testing we found the third harmonic was consistently correlated across channels, the image frequency was consistently uncorrelated, and the LO frequency varied depending on start-up conditions. This is reflected in Figure 3a, where we show coherent addition for the third harmonic, noncoherent addition for the image frequency, and partially coherent addition for the LO leakage frequency.

In Figure 7 and Figure 8, the transceiver LOs are all set to different frequencies and the digital NCOs are adjusted in both frequency and phase such that the signals coherently combine. In this case, the spurious signals produced from the image, the LO leakage, and the third harmonic are forced to be at different frequencies. Figure 7 shows the individual transmit outputs

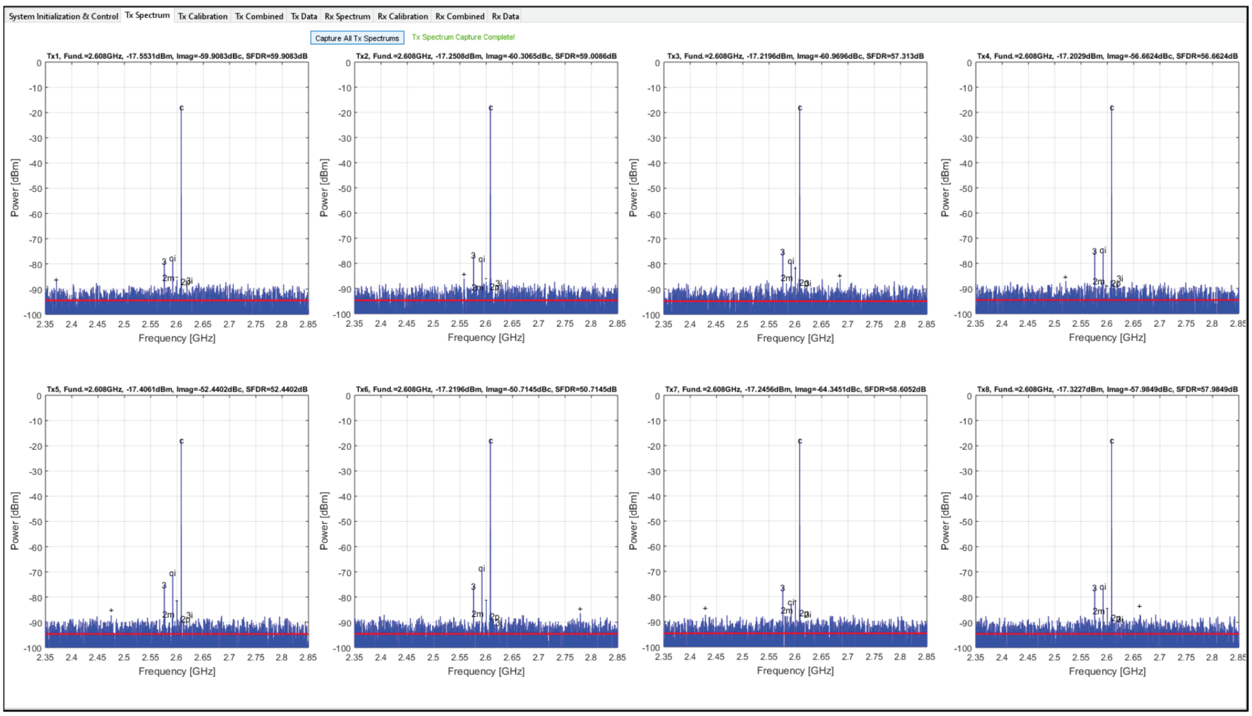

Figure 5. Waveform generator spurious of each channel with LOs and NCOs set to the same frequency.

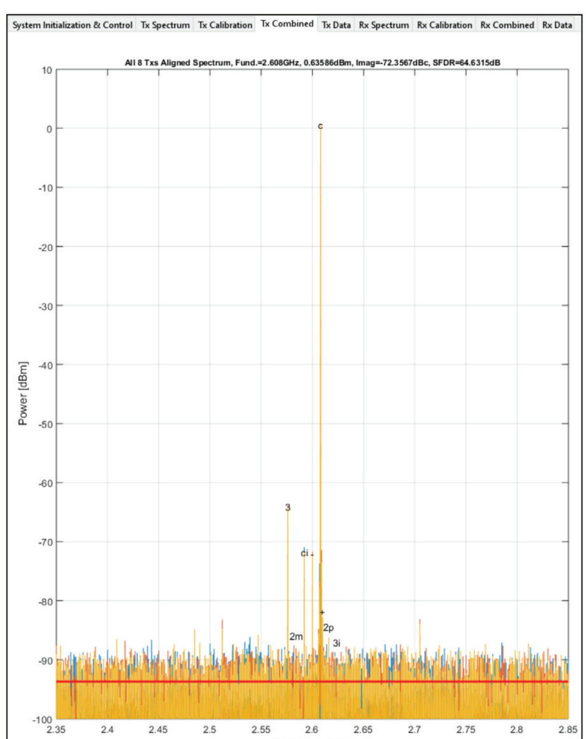

Figure 6. Combined waveform generator spurious with LOs and NCOs set to the same frequency. Note there is no improvement to the third-harmonic spur in this configuration.

measured on a spectrum analyzer. Figure 8 shows the combined output. In this test the spurs of the image, the LO leakage, and the third harmonic measured in dBc relative to the carrier begin to spread into the noise and every spur shows an improvement when channels are combined.

When a very small number of channels are combined, as was done in this test, the spurs actually show a 20log(N) improvement in their relative levels. This is due to the signal components combining coherently and adding as 20log(N) while the spurs do not combine at all. In practice, with a large array and a much greater number of channels being combined, the improvement is expected to approach 10log(N). This is for two reasons. First, with a large number of signals being combined it will not be practical to spread the spurs out sufficiently such that each one can be considered in isolation. Consider a 1 MHz modulation bandwidth as an example. If a specification says that spurious emissions are to be measured in a 1 MHz bandwidth, then ideally the spurs would be spread out so that they are at least 1 MHz apart. If this is not possible, then each 1 MHz of measurement bandwidth will include multiple spurious components. Since these will be at different frequencies, they will combine incoherently and the spurious power measured in each 1 MHz of bandwidth will increase

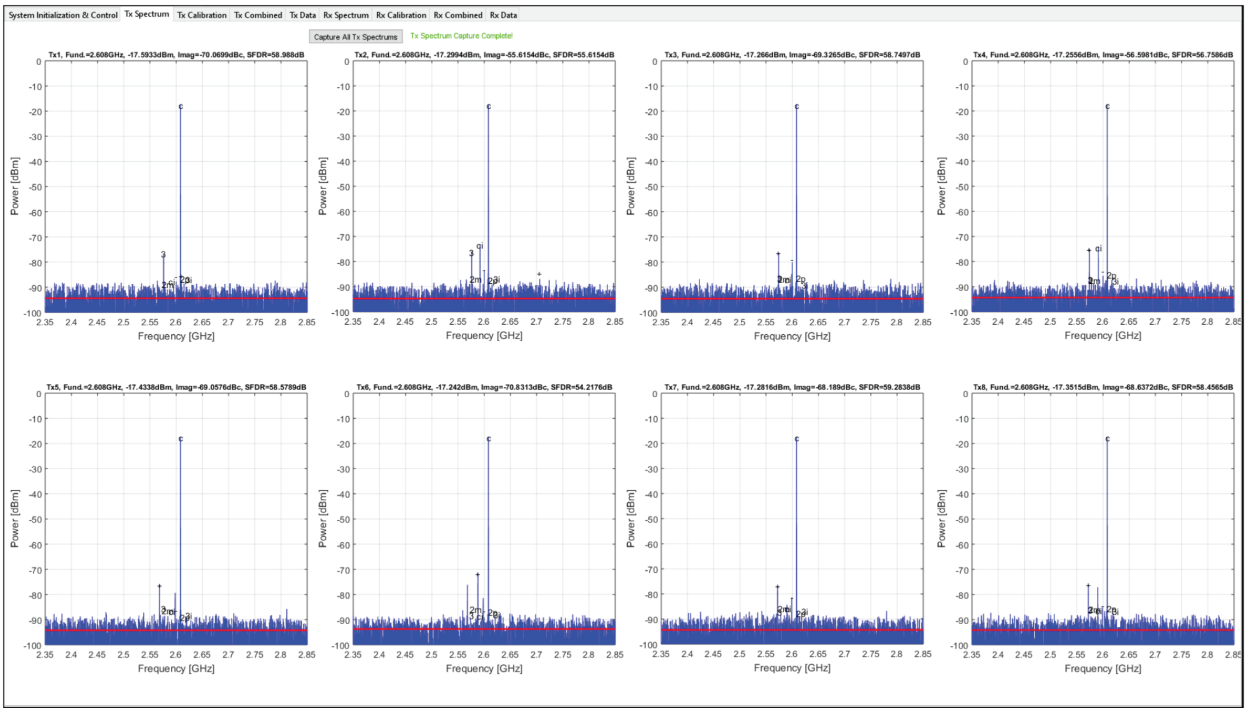

Figure 7. Waveform generator spurious of each channel with LOs and NCOs offset in frequency.

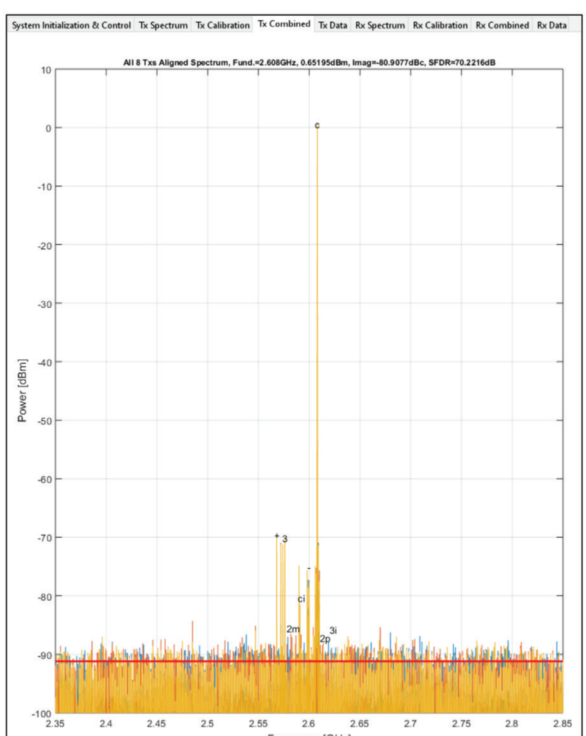

Figure 8. Combined waveform generator spurious with LOs and NCOs offset in frequency. Note in this case that the spurs are spread in frequency and there is a clear SFDR improvement relative to the individual channel SFDR.

as 10log(N). However, no single 1 MHz of measurement bandwidth will contain all the spurs, so in this case, N for the spurs is smaller than N for the signal and although the incremental improvement will be 10log(N), once N is large enough for the spurious density to place multiple spurs inside the measurement bandwidth, the absolute improvement will still be better than 10log(N) compared to the system without spurious signal decorrelation—that is, it will be somewhere between 10log(N) and 20log(N) decibels (or dB) better. Secondly, this test was done with CW signals, but real-world signals will be modulated and this will cause them to spread out, making nonoverlapping spurious signals impossible to achieve when a large number of channels are combined. These overlapping spurious signals will be uncorrelated and add incoherently, as 10log(N), in the overlap region.

It is worth making special mention of the LO leakage component when the LO is set to the same frequency across channels. The LO leakage is due to imperfect cancellation of the LO in the analogue modulator when two signal branches are summed. If the amplitude and phase imbalances are random errors, then the phase of the residual LO leakage component will also be random and when many different transceivers' LO leakages are summed they will add incoherently, as 10log(N), even when they are at precisely the same frequency. This should also be the case with the modulator's image component, but not necessarily the modulator's third harmonic. With a small number of channels being coherently combined, it is unlikely the LO phases would be completely random, and thus the cause for partial decorrelation is shown in the measured data. With a very large number of channels, the LO phase approaches a much more random condition across channels and is anticipated to be an uncorrelated addition.

Conclusion

The measured SFDR results when the LOs and NCOs are offset in frequency, which clearly shows the spurious created is all at different frequencies and is not coherent in the combining process, thus ensuring an SFDR improvement as channels are combined. LO and NCO frequency control is now a programmable feature in the latest Analog Devices' transceiver products. The results demonstrate this feature can be exploited in phased array applications, which ensures an array-level SFDR improvement over single-channel performance.

References

[1] Lincoln Cole Howard and Daniel Rabideau. "Correlation of Nonlinear Distortion in Digital Phased Arrays: Measurement and Mitigation." 2002 IEEE MTT-S International Microwave Symposium Digest.

[2] Salvador Talisa, Kenneth O'Haever, Thomas Comberiate, Matthew Sharp, and Oscar Somerlock. "Benefits of Digital Phased Arrays." Proceeding of the IEEE, Vol. 104, No. 3, March 2016

[3] Keir Lauritzen. "Correlation of Signals, Noise, and Harmonics in Parallel Analog-to-Digital Converter Arrays." Ph.D. Dissertation, University of Maryland, 2009.

[4] Rabinkin, Song, "Front-End Nonlinear Distortion and Array Beamforming." Radio and Wireless Symposium (RWS) 2015 IEEE

[5] Peter Delos. "A Review of Wideband RF Receiver Architecture Options." Analog Devices, Inc., February 2017

Delos, Peter. "Can Phased Arrays Calibrate on Noise?" *Microwave Journal*, March 2018

Harris, Jonathan. "What's Up with Digital Downconverters—Part 1." *Analog Dialogue*, July 2016.

Harris, Jonathan. "What's Up with Digital Downconverters—Part 2." *Analog Dialogue*, November 2016.

Howard, Lincoln, Nina Simon, and Daniel Rabideau. "Mitigation of Correlated Nonlinearities in Digital Phased Arrays Using Channel-Dependent Phase Shifts." 2003 EEE MTT-S Digest.

About the Authors

Peter Delos is a technical lead in the Aerospace and Defense Group at Analog Devices in Greensboro, North Carolina. He received his B.S.E.E. from Virginia Tech in 1990 and M.S.E.E. from NJIT in 2004. Peter has over 25 years of industry experience. Most of his career has been spent designing advanced RF/analog systems at the architecture level, PWB level, and IC level. He is currently focused on miniaturizing high performance receiver, waveform generator, and synthesizer designs for phased array applications. He can be reached at *peter.delos@analog.com*.

Mark Robertson graduated from Cambridge University, UK, in 1990 with a degree in electrical and information sciences. He worked as an RF and analog circuit design engineer for various companies in the test and measurement, cellular phone, and cellular base station industries before joining Analog Devices in in Bath, UK as a systems engineer in 2012. He still likes to design real circuits whenever he can. He can be reached at *mark.robertson@analog.com*.

Mike Jones is a principal electrical design engineer with Analog Devices working in the Aerospace and Defense Business Unit in Greensboro, North Carolina. He joined Analog Devices in 2016. From 2007 until 2016 he worked at General Electric in Wilmington, North Carolina as a microwave photonics design engineer working on microwave and optical solutions for the nuclear industry. He received his B.S.E.E. and B.S.C.P.E. from North Carolina State University in 2004 and his M.S.E.E. from North Carolina State University in 2006. He can be reached at *michael.jones@analog.com*.

Analog Devices, Inc.
Worldwide Headquarters

Analog Devices, Inc.
One Technology Way
P.O. Box 9106
Norwood, MA 02062-9106
U.S.A.
Tel: 781.329.4700
(800.262.5643, U.S.A. only)
Fax: 781.461.3113

Analog Devices, Inc.
Europe Headquarters

Analog Devices GmbH
Otl-Aicher-Str. 60-64
80807 München
Germany
Tel: 49.89.76903.0
Fax: 49.89.76903.157

Analog Devices, Inc.
Japan Headquarters

Analog Devices, KK
New Pier Takeshiba
South Tower Building
1-16-1 Kaigan, Minato-ku,
Tokyo, 105-6891
Japan
Tel: 813.5402.8200
Fax: 813.5402.1064

Analog Devices, Inc.
Asia Pacific Headquarters

Analog Devices
5F, Sandhill Plaza
2290 Zuchongzhi Road
Zhangjiang Hi-Tech Park
Pudong New District
Shanghai, China 201203
Tel: 86.21.2320.8000
Fax: 86.21.2320.8222